Review of wave interaction with continuous flexible floating structures

Zhang, Min; Schreier, Sebastian

DOI
10.1016/j.oceaneng.2022.112404

Publication date
2022

Document Version
Final published version

Published in
Ocean Engineering

Citation (APA)
Zhang, M., & Schreier, S. (2022). Review of wave interaction with continuous flexible floating structures. *Ocean Engineering*, *264*, Article 112404. https://doi.org/10.1016/j.oceaneng.2022.112404

Ocean Engineering 264 (2022) 112404

Contents lists available at ScienceDirect

Ocean Engineering

journal homepage: www.elsevier.com/locate/oceaneng

Review

Review of wave interaction with continuous flexible floating structures

Min Zhang, Sebastian Schreier *

Delft University of Technology, Delft, Zuid-Holland, The Netherlands

ARTICLE INFO

Keywords:
Very large floating structures
Ice-related structures
Hydroelastic methods
Characteristic length
Very flexible floating structures
Föppl–von Kármán plate theory

ABSTRACT

Thin continuous flexible floating structures have been shown to have technical and economic advantages for Offshore Floating Photovoltaic (OFPV) installations. In terms of large horizontal dimensions compared to the wave length, these structures are similar to sea ice as well as Very Large Floating Structures (VLFS), e.g. as proposed for floating airports. In this paper, we reviewed the hydroelastic theory for sea ice and VLFS and assessed its applicability to the newly envisaged flexible floating structures. While VLFS and sea ice motion in waves are dominated by elastic deformations, their motion amplitudes are limited to the order of the structure thickness. Thin and flexible floating structures were found to be able to follow the wave motion with amplitudes far exceeding their thickness. Nonlinear theories like Föppl–von Kármán plate theory are required to model these structures. The significant contribution of nonlinear effects in the structural response and the large deformations in waves far exceeding the structural thickness lead to the definition of the new category of Very Flexible Floating Structures (VFFS).

1. Introduction

The environmental issues, such as global warming, sea-level rising and climate change, caused by the burning of fossil fuels have become more and more serious since industrial revolution. There is an urgent need to develop sustainable and clean energy for powering the low carbon future of the planet. Among the available renewable resources, solar energy is the most abundant inexhaustible energy to humankind. Besides, photovoltaic (PV) technology has experienced enormous growth and PV system has achieved world-wide acceptance over the past few decades. Land shortage is another problem of many coastal cities as nearly 40 percent of the world's population live within 100 km of the coast (UN, 2017). Considering the fact that over two third of the earth's surface is covered by ocean, ocean space utilization could be a good solution to release the land-use pressure. Combining with the development of solar energy, a promising option to tackle both the land and energy problem is to develop offshore floating photovoltaics (OFPV). The idea of OFPV is to install PV systems on seawater and not occupy land space.

OFPV technology is generally a combination of PV technology and the floating technology. Even though flexible OFPV has been proposed as cost-competitive concept and has recently been developed in nearshore, there is still a long way to go for commercial floating technology that can take kilometer size structures into rough offshore environments. The floating technology for OFPV requires that the structures have enough buoyancy to float themselves as well as the PV panels and are able to withstand strong wind, wave, and current loads in open seas. Additionally, proper mooring systems are needed to keep the system in place. Moreover, the efficiency and economic potentials in synergies of offshore solar and offshore wind as well as aquacultures indicated that OFPV plants are better constructed in combination with other marine systems (López et al., 2020; Zheng et al., 2020).

The challenges for the development of floating technology for OFPV are the determination of (1) structural deformations under harsh wave conditions, (2) the acting wave forces on the structures in the regime of strong hydroelastic interaction, and (3) the surrounding wave responses due to the existence of the structures.

OFPV is an emerging field of research and development in recent years, see e.g. Jamalludin et al. (2019), and many different structural concepts are proposed as support structures. Based on inland floating solar systems, which are primarily pontoon-based (Trapani and Santafé, 2015; Sahu et al., 2016), modular floating designs are extended to offshore applications, such as the projects of Oceans of Energy (2019) and the tank tests of connected triangular pontoons of Waals et al. (2018) and Otto et al. (2020). However, modular structures cause limitation on the size of plant and cannot withstand extreme environmental conditions as there will be large stress concentrations on the connection elements (Oliveira-Pinto and Stokkermans, 2020). Alternatively, a flexible floating system consisting of thin-film PV arrays was designed by Trapani et al. (2013) with focus on large-scale offshore solar development. Trapani's concept was based on a thin floating

* Corresponding author.
E-mail address: s.schreier@tudelft.nl (S. Schreier).

https://doi.org/10.1016/j.oceaneng.2022.112404
Received 4 August 2021; Received in revised form 19 August 2022; Accepted 22 August 2022
Available online 15 September 2022

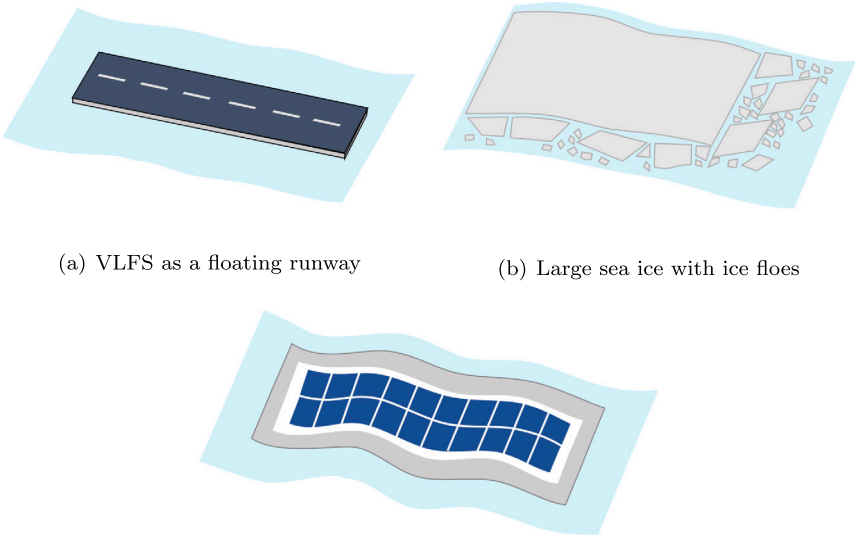

(a) VLFS as a floating runway

(b) Large sea ice with ice floes

(c) VFFS as a support of OFPV

Fig. 1. Concept sketch of VLFS, sea ice, and VFFS.

polymer layer with length and width of 600 m × 200 m. Compared to the pontoon-based type, the flexible approach is more commercially attractive due to the inherent flexibility allowing the system to easily deform with wave motions, leading to low wave forces acting on the structure and the moorings. This economic advantage of flexible floating support was also mentioned in the project of Ocean Sun (2018), where pre-stretched membranes of several millimeters thin are used for mounting rigid PV panels. More recently, Solar@Sea I & II test showed the potential of floating, non-rigid thin-film PV modules for large-scale PV installations (Soppe, 2020). The continuous flexible system is suitable for utility-scale structures of square kilometer in size—either as a single structure or in a combination of modules.

Considering flexible support for OFPV, Schreier and Jacobi (2020) conducted experiments with a very flexible floating sheet subjected to regular waves. They found that their flexible sheet mainly followed the local wave elevation and the vertical deflections were large compared to the structure thickness, which was different from the motion of VLFS and sea-ice where deflections were mostly in the same order of the thickness.

Structures with square kilometer in horizontal size have been studied before for floating runway Mega-Float (Suzuki, 2005) and in sea-ice research. The newly proposed structures have much smaller thickness to horizontal dimensions ratio, leading to low bending stiffness in the vertical direction, and thus making the structure very flexible under wave actions. Fig. 1 illustrates the concept of VLFS, sea ice, and VFFS.

With very large horizontal dimensions compared to their structural thickness, there are parallels between flexible floating structures for OFPV support and pontoon-type VLFS (Wang and Tay, 2011) as well as sea-ice (Squire, 2008). According to Suzuki et al. (2006), elastic deformation are the governing response of those structures in waves.

There are currently not many investigations available regarding very flexible support systems for OFPV. Therefore, based on the similarities between flexible OFPV structures and VLFS and sea-ice, numerical and experimental studies were reviewed in this paper to assess the applicability of employed theories as well as experimental and numerical techniques to these newly proposed structures. The analytical consideration of the hydro-elastic problem is described in Section 2. The review of previous works is presented in Section 3. Section 4 analyses the previous work and gives a characterization of the investigated structures. The applicability of the available theory is discussed in Section 5, and concluding remarks are given in Section 6.

2. Analytical consideration of the hydro-elastic response

Compared to other marine structures, VLFS and sea ice have two distinct hydrodynamic features. One feature is that the structures have large horizontal dimensions of several kilometers and rather small vertical size of only a few meters, thus resulting in very small bending rigidity in vertical direction. The other one is that the wavelengths of practical interest are small compared to the structure length. These two features make the elastic behavior more important than rigid body motion (Suzuki et al., 2006).

2.1. Analytical models

Due to their large horizontal dimensions and a small vertical one, VLFS and sea ice are often regarded as mat-like structure resting on water surface and modeled as a thin elastic plate with zero thickness. The hydro-elastic problem is usually simplified to be a linear problem by assuming both the incident wave amplitude and the structure displacement are small. The classic thin plate theory (also known as Kirchhoff plate theory) is thus being used to describe the vibration of the floating body. The governing equation is given as

$$D\nabla^4 W + m\frac{\partial^2 W}{\partial t^2} + \rho g W = P \tag{1}$$

where ∇ is the vector differential operator defined as $\nabla = (\frac{\partial}{\partial x}, \frac{\partial}{\partial y})$; $D = \frac{EI}{1-\nu^2}$ is the plate rigidity with E Young's modulus, I cross-sectional area moment of inertia per unit width and ν Poisson's ratio; m is the mass per unit area of the plate; ρ is the density of the fluid; g is the gravitational acceleration; $P = P(x, y, t)$ is the dynamic pressure on the bottom surface of the plate. The pressure P relates to the velocity potential $\Phi = \Phi(x, y, z, t)$ at the bottom surface of the plate by

$$P = -\rho\frac{\partial \Phi}{\partial t} \tag{2}$$

and $W = W(x, y, t)$ is the complex vertical displacement of the plate satisfying the boundary condition at the bottom surface of the plate by

$$\frac{\partial W}{\partial t} = \frac{\partial \Phi}{\partial z} \tag{3}$$

For simplicity, considering an elastic floating body with zero-draft subjected to linear regular wave, and assuming all motions are time-harmonic with the common time dependence $e^{i\omega t}$ applied to all first order oscillatory quantities, the velocity potential becomes $\Phi(x, y, z, t) =$

$\Re\{\phi(x,y,z)e^{i\omega t}\}$, and the first order vertical displacement of the plate becomes $W(x,y,t) = \Re\{w(x,y)e^{i\omega t}\}$, where $\Re$ represents the real value; i is the imaginary unit; ω the angular frequency; and t the time. Substituting Eqs. (2) and (3) into Eq. (1), and factoring all quantities by ρg, the governing equation then becomes

$$\left(1 - \frac{m\omega^2}{\rho g} + \frac{D}{\rho g}\nabla^4\right)\frac{\partial \phi}{\partial z} = \frac{\omega^2}{g}\phi \tag{4}$$

This equation can be seen as a modified free surface boundary condition with consideration of floating plate properties that are different from water waves. When $m = 0$ and $D = 0$, it becomes the free surface condition of open water wave.

2.2. Hydro-elastic dispersion relation

From the modified free surface condition, i.e. Eq. (4), the dispersion relation of elastic waves of a thin plate can be expressed as (Ohmatsu, 2005)

$$\left[1 - \frac{m\omega^2}{\rho g} + \frac{Dk_b^4}{\rho g}\right] k_b \tanh k_b h = \frac{\omega^2}{g} \tag{5}$$

or an alternative form

$$\left[1 - \left(\frac{\omega}{\omega_0}\right)^2 + \left(\frac{k_b}{k_c}\right)^4\right] k_b \tanh k_b h = \frac{\omega^2}{g} \tag{6}$$

where h is the water depth, $\omega_0 = \sqrt{\rho g/m}$ is the heave natural frequency of the dry plate, k_b represents the hydro-elastic wave number and $k_c = (\rho g/D)^{1/4}$ represents the characteristic wave number of the plate.

If $m = 0$ and $D = 0$, Eq. (5) or Eq. (6) becomes the dispersion relation of open water wave

$$k_w \tanh k_w h = \frac{\omega^2}{g} \tag{7}$$

In case of wave propagating to a floating plate with $m \neq 0$ and $D \neq 0$, the hydro-elastic wave number is theoretically determined by term $C = \left[1 - \left(\frac{\omega}{\omega_0}\right)^2 + \left(\frac{k_b}{k_c}\right)^4\right]$.

When $C = 1$, i.e. $\left(\frac{\omega}{\omega_0}\right)^2 = \left(\frac{k_b}{k_c}\right)^4$, the hydro-elastic wave number k_b is equal to the open water wave number k_w: $k_b = k_w$. The hydro-elastic wavelength is the same as the propagating wavelength.

When $C < 1$, i.e. $\left(\frac{\omega}{\omega_0}\right)^2 > \left(\frac{k_b}{k_c}\right)^4$, the hydro-elastic wave number k_b is larger than the open water wave number k_w: $k_b > k_w$. The hydro-elastic wavelength is thus shortened by the elastic floating structure.

When $C > 1$, i.e. $\left(\frac{\omega}{\omega_0}\right)^2 < \left(\frac{k_b}{k_c}\right)^4$, the hydro-elastic wave number k_b is smaller than the open water wave number k_w: $k_b < k_w$. The hydro-elastic wavelength is thus lengthened by the elastic floating structure.

As the wave energy should be continuous at the side of the structure, the change in wavelength underneath the structure would result in the direction of wave celerity changing accordingly, as shown in Fig. 2. Physically speaking, when wave shortens, the outside wave would enter into the hydro-elastic zone which causes wave focusing, whereas wave lengthens, the wave would exit from the hydro-elastic zone which causes wave spreading. Note that wave shortening could cause unexpected large deformation of the structure due to wave energy increases beneath.

2.3. Structural stiffness

As shown in Eq. (6), k_c is an important parameter to quantify the effect of structural bending stiffness on hydro-elastic response. In this study, for the purpose of an intuitive comparison to the length scales, the characteristic length $\lambda_c = 2\pi/k_c$ instead of k_c is used. λ_c was firstly proposed by Suzuki and Yoshida (1996) and the equation was given in Eq. (8) by Suzuki et al. (2006) based on beam results.

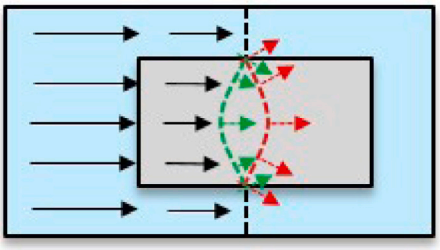

Fig. 2. Schematic of wave focusing (green) and spreading (red). (For interpretation of the references to color in this figure legend, the reader is referred to the web version of this article.)

$$\lambda_c = 2\pi\left(\frac{EI}{\rho g}\right)^{1/4} \tag{8}$$

here EI is the bending stiffness of the beam per unit width. The product ρg is the hydro-static stiffness of structure per unit width. The λ_c is the characteristic length of the elastically supported beam and can be interpreted as the length affected by a localized load. Suzuki et al. (1997) defines VLFS not only as floating structures with large horizontal dimensions compared to wavelength of practical interest, but also as having lengths larger than the characteristic length.

For comparison purposes, plate and beam structures were characterized by λ_c, where the plate bending stiffness is converted to $EI = D(1-\nu^2)$ and the characteristic length of a plate is expressed as $\lambda_c = 2\pi(D/\rho g)^{1/4}$.

3. Review of VLFS and sea ice studies

Floating technology has received significant attention among industry and research as VLFS have been foreseen as promising alternatives to relieve the vigorously growing pressure on land use for population accommodation and industrial expansion (Wang and Tay, 2011; Lamas-Pardo et al., 2015). However, although the concept of VLFS has been introduced over 100 years ago and the floating technology has achieved great improvement since the 1990s, real VLFS are still yet to come due to their distinct structure size and the complex interaction with waves. To predict the hydro-elastic response of these structures in waves, many analytical or numerical, and experimental studies have been carried out over the past few decades. In this section, the common methods used to solve the wave–structure coupled equation (Eq. (1)) are firstly outlined, the numerical and experimental studies in VLFS and sea-ice are then reviewed.

3.1. Numerical studies

As shown in Eq. (1), the motion of the structure is governed by a fourth-order partial differential equation, the analytical solutions of these equations are essentially impossible to achieve except in some one-dimensional cases. Alternatively, numerical studies are used and developed along the evolution of floating technology. Over the decades, different numerical approaches to the hydro-elastic problem have been proposed and a variety of structures have been investigated.

3.1.1. Hydroelastic methods

Pioneering work of hydroelasticity theory was done by Bishop et al. (1979) and Mei and Tuck (1980) for 2-dimensional model and Wu (1984) for 3-dimensional analysis. Early applications of hydroelastic theory to large floating structures include Langen and Sigbjörnsson (1980) and Georgiadis (1981) for "beam-like" structures as well

as Price and Wu (1985) and Wu and Du (1990) for complex structures of arbitrary geometry.

Regarding the nature of solution in the structure, a decision must be made by choosing a method in one of two broad categories (Ohmatsu, 2005). The first set of option is the modal expansion method. In this method, the structure motion and the hydrodynamics are solved separately. The structure motion is approximated by a summation of the product of modal functions and their complex amplitudes, while the hydrodynamic part can be obtained through Green's integral method or eigenfunction expansion-matching method. The coupling is then achieved by evaluating the hydrodynamic forces on the structure for unit amplitude motions of each mode. The second family is the so-called direct method, in which the velocity potential is directly obtained by solving the coupled equation of motion without the help of modes and the structure motion is then estimated from the resultant potential.

Using modal expansion method to solve hydroelastic problem has a very long history, early full description of this method can be found in the work of Bishop et al. (1979) and Wu (1984). Later, as VLFS received high interest among industry and academia, modal expansion method was widely used in the hydrodynamic analysis of beam-like or pontoon-type VLFS due to its simplicity of determining motion vibration (Wu et al., 1995, 1996; Kashiwagi, 1997, 1998a; Hermans, 2000; Abul-Azm and Gesraha, 2000; Meylan, 2002; Andrianov, 2005; Montiel, 2012; Karmakar and Soares, 2012; Praveen et al., 2018, 2020). Along the development of this method, various types of modal functions have been proposed, including modes of a finite free–free beam (Gran, 1992; Newman, 1994; Maeda et al., 1995; Taylor and Ohkusu, 2000), finite plate with free edges (Meylan and Squire, 1996; Meylan, 2002), infinite or semi-infinite beam and plate (Hermans, 2000; Andrianov, 2005), and B-spline functions (Kashiwagi, 1997, 1998a). The modes may be of the dry type considering structure vibration in vacuum or wet type including the fluid effect on the modes shapes calculation (Taylor, 2003; Loukogeorgaki et al., 2012). Most researchers used the dry-mode approach because these modes are easily specified in advance by applying the orthogonality properties.

In the line of direct method, early procedures developed by Mamidipudi and Webster (1994) and Yago (1997) using Green's function of the water surface to solve the wave components and the finite difference/element scheme to obtain the structure motion were shown to be time and memory consuming for the calculation of wave interaction with a large floating structure. To avoid those disadvantages, Ohkusu and Nanba (1996) introduced a different direct method for pontoon-type VLFS based on the analytical approach of sea ice proposed by Evans and Davies (1968) and Meylan and Squire (1994). The idea of this approach is to treat the floating structure as part of the water surface but with different physical properties, thus replacing the structure mechanics problem of determining the elastic motion of the body due to wave actions by a boundary-value problem in hydrodynamics. The Green's function of the floating cover is used rather than that of the free water surface. To reduce the computation time of Green's function integration over the wet surface of the structure, Ertekin and Kim (1998) proposed an efficient expansion matching approach based on the direct method by using eigenfunctions of the wave to estimate the velocity potential rather than integrating Green's function of the structure over the entire wet surface. They showed that their approach is efficient for parametric study of hydroelastic response of pontoon-type VLFS because the discretization of the structure was needed only along its edges rather than on the entire pontoon in usual panel methods, replacing the time-consuming evaluation of the area integral by efficient line integrals. Kim and Ertekin (2000) and Hong et al. (2003) modified this approach by accounting for finite draft effect on the structure behavior.

Comparison work of modal expansion method and the direct method was done by Taylor (2007). Results showed that the modal expansion method overestimated the effect of hydrodynamic forces but it was more lucid and time-efficient in computation than the direct method, but for large and flexible structures, massive numbers of modes might be needed. Additionally, calculations of wave quantities was not straightforward in modal expansion method. Moreover, the direct method avoids the error induced by truncating the series expansion of the modal expansion method. However, the direct method leads to much larger system of unknowns and for high frequency motions, the expression of Green's function of the structure was badly conditioned, limiting the application of the approach to comparatively stiff structures, like ice floes. Hegarty and Squire (2008) further points out that the method based on Green's function of the structure did not converge to higher-order deflections. The pros and cons of the hydroelastic methods are summarized in Table 1

Across the modal expansion method and the direct method, the hydro-elastic problem is addressed by boundary element method (BEM) finite element method (FEM), or the hybrid BEM-FEM. In general, BEM traditionally gained a degree of popularity on a basis of efficiency. Because in BEM the partial differential equations are formulated as integral equations using Green's function method and the given boundary conditions of the problem are used to fit the boundary values into the integrals, rather than values throughout the space. Therefore, only the surface, rather than the entire volume, needs to be discretized in simulation, which leads to the reduction of spatial dimensions of the problem by one, and a smaller system of equations in the computation program. Particularly, BEM is well-suited to problems with infinite or semi-infinite domain (see e.g. Hermans, 2000; Andrianov and Hermans, 2006). Whereas in FEM, problem domain of interest is divided into collection of finite sub-domains (finite elements) and the concept is to represent the geometry of each single sub-domain by applying proper boundary conditions and loads. A variety of different finite element formulations has been proposed over the years to modal problems of various complexity.

However, due to volume discretization in FEM, the system of equations could be considerably large due to the higher number of degrees of freedom in the system. Besides, FEM can be very computationally expensive as the stability of FEM is highly dependent on the mesh quality, a very fine mesh is required for accurate prediction. By contrast, there are far less elements in BEM because of surface discretization. Although BEM gives full matrices whereas FEM leads to narrow brand ones, a full BEM matrix usually still solves faster than a sparse FEM matrix. One major limitation of BEM is its less successful application to nonlinear problems (Wu and Taylor, 2003), but higher-order BEM (HOBEM) could be an option (Heo and Kashiwagi, 2019, 2020).

To make use of the advantages of BEM and FEM, a hybrid BEM-FEM technique has been developed in which the BEM is used to discretize the fluid field and FEM is used to discretize the floating structure. Early BEM-FEM procedure applied in VLFS can refer to e.g. Utsunomiya et al. (1995), Yasuzawa (1996), Yago (1997) and Hamamoto et al. (1997). Further improvement to higher-order BEM-FEM approach respecting computational efficiency and accuracy has been continuously proposed in the field of hydroelasticity (e.g. Kashiwagi, 1998c; Wang and Meylan, 2004; Yoon et al., 2014; Shirkol and Nasar, 2018, 2019) .

3.1.2. Application of hydroelastic method

Modal expansion method has been used extensively over the past decades. Wu et al. (1995) conducted a 2-dimensional analysis of an experimental model of 10 m by 0.5 m by 0.038 m with $\lambda_c = 2.92$ m. The structure motion was estimated by the free–free beam modes proposed by Newman's (Newman, 1994). The wave field was approximated by wave eigenfunctions. This solution is also called the eigenfunction expansion-matching method (EEMM). Acceptable agreement of the calculated displacement and bending moment results with experimental values was obtained. Then Wu et al. (1996) extended the application of the modal expansion method to 3-dimensional box-like pontoons with dimensions of 300 m by 60 m by 2 m and 4000 m by 1250 m by 4.5 m. The wave field was solved by using the water surface Green's function.

Table 1
Overview of pros and cons of hydroelastic methods.

Method	Pros	Cons
Modal expansion method	–lucid procedure –time and memory efficient	–overestimates hydrodynamic forces –many modes needed for large and very flexible structures –prone to modes truncation error
Direct method	–straightforward calculation –no modes truncation error	–large number of unknowns –badly conditioned Green's function in very flexible structures –convergence problem in higher-order deflections

Comparisons between 2-dimensional results and 3-dimensional results indicated that the 2-dimensional approach overestimated the global response and for short wavelengths, where the 3-dimensional analysis was recommended. Kashiwagi (1997) applied the modal expansion method with cubic B-spline functions on a floating elastic plate of 5000 m long, 1000 m wide and 5 m thick with a characteristic length of 782 m in the regime of very short wavelengths. Satisfactory results were obtained up to $L/\lambda = 50$, with feasible computation time and the number of unknowns for routine use. Ohmatsu (1997) investigated the hydroelastic behavior of typical VLFS with various lengths ranging from 1200 m to 4800 m subjected to rather short waves using EEMM. Chen et al. (2003) used modal expansion method with Green's integrals to address the large-amplitude response problem of a pontoon-type VLFS treated as a floating plate of 300 m × 60 m × 2 m with λ_c = 188 m in monochromatic and multi-directional waves. Worth noting that in this work, they provided a nonlinear hydroelastic solution that accounted for geometric characteristics of the structure in short waves using Föppl–von Kármán plate theory. Detailed description of the problem solution accounting for the geometric nonliterary can be found in Chen et al. (2004). The nonlinear membrane forces induced by large deflections were calculated. Comparison between linear and nonlinear results indicated that membrane forces had little effect on the motion response, but increased the longitudinal stress by 30% in the case of monochromatic waves. Watanabe et al. (2006) proposed a benchmark analysis of circular VLFS using modal expansion method. Radius of 50 m and 200 m with thickness 5 m and 2 m were considered in their work. Response of deflection, bending moment, twisting moment and transverse shear force were calculated. Gao et al. (2011) addressed the hydroelastic problem of a hinged thick VLFS by applying the modal expansion method to the structure and the boundary element to the fluid domain. Tay and Wang (2012) conducted a numerical investigation of floating plates of 300 m by 60 m by 2 m and 150 m by 150 m by 2 m with various fore- and aft-end shapes in regular waves using modal expansion method with boundary integrals. More recent, the application of the modal expansion method can be found in motion prediction of various complicated floating structures proposed to meet different engineering needs, such as modular VLFS (Yang et al., 2019; Ding et al., 2020), VLFS with different support conditions (Praveen et al., 2019), floating VLFS with submerged plates (Mohapatra and Guedes Soares, 2016; Mohapatra and Soares, 2019), VLFS with anti-motion device (Cheng et al., 2016; Singla et al., 2019; Pu and Lu, 2022), circular flexible VLFS (Heo and Kashiwagi, 2020; Meylan, 2021). Wave interaction with sea ice shares the same fundamental mathematical model with wave-VLFS interaction (Squire, 2008). Modal expansion method can be also applied to the hydroelastic analysis of wave–ice coupling problem, such as Meylan (2002), in which the wave-induced motion of a flexible ice floe of rectangular, diamond, trapezoid and triangular shape was calculated based on modes approximation method. But for wave propagation through ice floes, multiple ice floes should be considered. For hydroelasticity of multiple ice floes, the wave scattering between the ice floes should be included, modal expansion method may not be a good choice since it has a drawback of estimating wave scattering. Here we keep our focus on continuous structures so multiple ice floes are omitted. The reader is referred to the latest overview by Squire (2020) for multi-structure models of ice-related research.

For the direct method, the early application on hydroelastic analysis can be found in the problem of wave–ice coupling (Evans and Davies, 1968; Meylan and Squire, 1994). Meylan and Squire (1996) investigated the hydroelastic response of circular ice floes represented by circular disks to long-crested ocean waves using the direct method, in which Green's function of the ice cover was adopted. Their models had various radii from 50 m to 400 m and a constant thickness of 0.5 m with a characteristic length of 57.1 m. To improve the computational efficiency of the direct method, Athanassoulis and Belibassakis (1999) proposed a coupled-mode method to address the coupling equation by introducing the series expansion of wave field into variational principle rather than using the integral approach. Belibassakis and Athanassoulis (2005) addresses the hydroelastic problem of large floating structures over different bathymetry conditions using a coupled-mode model. Studies on the hydroelastic response of a 500 m long floating ice sheets with small draught and variable thicknesses in different slopping bathymetry conditions were conducted in the work of Belibassakis and Athanassoulis (2005) and Belibassakis et al. (2013). In VLFS study, based on the idea of treating the floating structure as part of the water surface but with different physical characteristics, Ohkusu and Nanba (1996) extended the application of method proposed by Meylan and Squire (1994) to wave-VLFS study. Ertekin and Kim (1999) analyzed the hydroelastic response of a 5000 m by 1000 m by 5 m floating runway in regular, oblique, shallow water waves by the direct method. Effects of stiffness, structure length and width on structure deflections, wave reflection and transmission were discussed. Ohkusu and Namba (2004) studied the bending vibration of a large thin floating plate of 5000 m by 1000 m by 5 m with a characteristic length of 420 m in monochromatic waves of 100 m to 250 m long using the direct method. However, Green's function of the structure is badly conditioned for higher-order deflections and high frequency motions limiting the application of the direct method to relatively stiff structures. For more complicated cases of wave floating structures interaction, the most popular solution is BEM-FEM, such as Yoon et al. (2014), Lu et al. (2016), Shirkol and Nasar (2019), Luong et al. (2020), Nguyen et al. (2020) and Jiang et al. (2021).

An overview table of VLFS numerical models is provided in Table 2. Because for large ice structure simulations, infinite or semi-infinite models were usually used and the thickness information was often not given, it is difficult to generate the overview table of numerical ice research in the same pattern of Table 2. Hence the table of numerical ice models is omitted.

3.2. Experimental studies

In analytical or numerical prediction, assumptions made to make the problem calculable may ignore some important physics, and the predicted results may be different from the actual cases. It is therefore crucial to conduct experiments of elastic floating structures to validate the theoretical analysis and also investigate the structure behavior in real conditions.

Table 2
Models used in VLFS simulations.

$L \times B \times h$ [m^3]	λ_c [m]	λ [m]	Reference
$300 \times 60 \times 2$	104 – 1846	55.4 – 343	Wu et al. (1996)
$4000 \times 1250 \times 4.5$	628 – 19 842	359 – 508	Wu et al. (1996)
$1200 - 4800 \times 1000 \times 2$	338	38.9 – 271	Ohmatsu (1997)
$5000 \times 1000 \times 5$	782	111 – 250	Kashiwagi (1997)
$5000 \times 1000 \times 5$	418	125 – 250	Ertekin and Kim (1999)
$1200 \times 240 \times 1$	288	60.0 – 216	Ertekin and Kim (1999)
$5000 \times 1000 \times 5$	418	250 – 1000	Hong et al. (2003)
$300 \times 60 \times 2$	188	50.0	Chen et al. (2003)
$5000 \times 1000 \times 5$	420	100 – 250	Ohkusu and Namba (2004)
R 50 × 5	287	50.0	Watanabe et al. (2006)
R 200 × 2	181	50.0	Watanabe et al. (2006)
$300 \times 60 \times 2$	188	60.0 – 300	Gao et al. (2011)
$150 \times 150 \times 2$	188	30.0 – 150	Tay and Wang (2012)
$300 \times 60 \times 2$	188	60 – 420	Yoon et al. (2014)
$400 \times 60 \times 3.7$	304	–	Cheng et al. (2016)
$300 \times 60 \times 2$	188	120 – 420	Lu et al. (2016)
R 1	3.528 – 4.196	–	Heo and Kashiwagi (2020)
R 2 (dimensionless)	0.628 – 3.533	2.09	Meylan (2021)

R: the radius of the structure.

Table 3
Law of similarity.
Source: Adapted from Ohmatsu (2008).

Geometrical condition	$L_m = \alpha L_f$
Mass per unit area	$M_m = \alpha M_f$
Time condition	$T_m = \sqrt{\alpha} T_f$
Vertical bending rigidity	$(\lambda_c)_m = \alpha(\lambda_c)_f$

α: the geometric scale ratio; m: model scale; f: full scale.

3.2.1. Law of similarity

In practice, full-scale structure experiments on large floating structures are generally not possible, so model-scale structures are alternatively used. Reasonable conversion from results of model-scale structure to results of full-scale structure can be achieved by satisfying the similarity law. In linear regime, the motion of full structure and experimental model should satisfy the equation of motion (Eq. (1)) and the dispersion relation (Eq. (6)). For a floating structure with a very large horizontal size and a rather small vertical one, elastic body motion is dominant in the structure behavior (Suzuki et al., 2006). Hence bending rigidity similarity between the model and the actual structure is necessary to be considered. Ohmatsu (2008) gives the list of similarity conditions related to the hydro-elastic response of VLFS based on the derivation results of Endo (1991). Among them, the parameters of similarity in Table 3 are important in VLFS experiments.

However, it is often very difficult to satisfy the similarity law of bending rigidity in VLFS. Because if only consider the geometric scaling, the rigidity per unit width in the model by definition is scaled by α^3 which does not match with the result derived from the equation of motion, where the rigidity should be scaled by α^4. Therefore, different materials and fabricating methods have to be used to simultaneously satisfy the similarity condition of mass and bending rigidity between model-scale structures and full-scale structures (Ohmatsu, 2008).

3.2.2. Experimental studies of VLFS

A significant milestone of VLFS development was the construction of the Mega-Float from 1995 to 2001 with intended full-scale dimensions of 5000 m × 1000 m and structural thickness of 5 m (Kashiwagi, 1997). This development provided the possibility of onsite experiments of large floating models. During this time, several experiments related to the Mega-Float project were reported. Utsunomiya et al. (1995) carried out experiments of a model with length of 10 m, width of 0.5 m and various thicknesses of 0.019 m, 0.038 m and 0.076 m, corresponding to characteristic lengths of 1.75 m, 2.94 m and 4.95 m, respectively, to investigate the effect of structural stiffness on structure deformations. Regular waves with periods of 0.6 s to 2.86 s and wave height from 0.005 m to 0.020 m were applied. They concluded that the influence of structural flexibility on the wave response of a large floating structure was significant and the consideration of structural flexibility would result in a more commercial design in a flexible floating structure. Yago and Endo (1996) investigated a 9.75 m long, 1.95 m wide model with a thickness of 0.0545 m and a characteristic length of 6.15 m related to a full-scale structure of 300 m by 60 m by 2 m with characteristic length 188 m. The longitudinal distributions of vertical displacement amplitudes and bending moment amplitudes along the centerline were reported for different wave periods and incident angles. Their model was later used in the work of Ohmatsu (1997) and Hamamoto and Fujita (2002) for the purpose of numerical solutions validation. In the study of Ohmatsu (1997), experiments of another longer elastic model with length of 15 m, width of 3 m, thickness of 0.056 m and a characteristic length of 3.63 m were also documented. Kagemoto et al. (1998) tested a 2 m long, 0.5 m wide, 0.005 m draft model consisting of 100 buoyant rectangular solids attached to a flexible upper deck of 0.005 m acrylic glass. Maeda et al. (2000) investigated a model of 4 m long, 1 m wide with thickness of 0.03 m and characteristic length of 1.31 m under long-crested irregular waves and two-directional irregular waves. The conditions of head sea, beam sea and oblique sea were used. Liu and Sakai (2002) carried out 2D experiments of polyethylene plates of 10 m long, 0.010 m and 0.020 m thick with characteristic length of 1.68 m for the thinner model and 2.83 m for the thicker one subjected to regular, random and solitary waves. Shiraishi et al. (2003) experimentally analyzed the elastic response and mooring forces of a VLFS moored inside a coastal reef in a 3D wave basin. They used a model of 12 m long, 1.2 m wide and 0.04 m thick with a draft of 0.008 m and a characteristic length of 15.64 m to simulate a full-scale structure of 1500 m by 150 m by 5 m with characteristic length 120 m. Li et al. (2003) conducted a model test with a model consisting of 0.045 m foamed polyethylene attached to a 0.005 m aluminium plate. The model length, width, height and draft were 10 m, 1.0 m, 0.05 m and 0.02 m respectively with a characteristic length in the longitudinal direction of 3.10 m. Regular waves of wave height 0.02 m and six wave periods between 0.80 s and 2.53 s were considered. Takagi and Nagayasu (2007) presented a small-scale model with horizontal size of 1.2 m by 0.4 m and a thickness of 0.1 m for the purpose of numerical method validation. Pham et al. (2009) documented an experimental study on various devices to reduce heave motion of a VLFS model with length 2.44 m, width 0.5 m, height 0.06 m and a characteristic length 2.33 m. Ohmatsu (2006) summarized the necessity of conducting experimental studies and gave an overview of the experimental methods employing large-scale models in wave basins. He concluded that experimental research is of great importance to the development of the floating technology. More recently, Yoon

Table 4
Models used in VLFS experiments.

$L \times B \times h$ [m^3]	λ_c [m]	λ [m]	Reference
$10.0 \times 0.50 \times 0.019$, 0.038, 0.076	1.75, 2.94, 4.95	0.56 – 8.54	Utsunomiya et al. (1995)
$9.75 \times 1.95 \times 0.0545$	6.15	1.00 – 8.61	Yago and Endo (1996)
$15.0 \times 3.00 \times 0.056$	3.63	0.75 – 2.10	Ohmatsu (1997)
$2.00 \times 0.50 \times 0.005$	1.48	0.39 – 6.25	Kagemoto et al. (1998)
$4.00 \times 1.00 \times 0.030$	1.31	–	Maeda et al. (2000)
$10.0 \times 0.80 \times 0.01, 0.02$	1.68, 2.83	0.39 – 6.25	Liu and Sakai (2002)
$12.0 \times 1.20 \times 0.04$	15.64	2.44 – 4.05	Shiraishi et al. (2003)
$10.0 \times 1.00 \times 0.05$	3.10	1.00 – 6.14	Li et al. (2003)
$1.20 \times 0.40 \times 0.0001$	0.09	0.072 – 0.146	Takagi and Nagayasu (2007)
$2.44 \times 0.50 \times 0.06$	2.33	1.00 – 2.64	Pham et al. (2009)
$3 \times 0.6 \times 0.04$	6.13	1.8	Yoon et al. (2014)
$8 \times 1.2 \times 0.0736$	1.68	–	Cheng et al. (2016)
$4.95 \times 1.02 \times 0.005$	0.17	0.495 – 0.99	Schreier and Jacobi (2020)

et al. (2014) carried out laboratory experiments with a 3 m long, 0.6 m wide, and 0.04 m thick VLFS with $\lambda_c = 6.13$ m subjected to regular waves with a wavelength 1.8 m and four different angles. Cheng et al. (2016) investigated the hydroelastic response of an 8 m by 1.2 m by 0.0736 m VLFS model with $\lambda_c = 6.09$ m edged with dual inclined perforated anti-motion plates subjected to irregular waves according to a JONSWAP spectrum. Waals et al. (2018) described a conceptual test of a modular diamond-shaped floating mega island. The structure consisted of 7 larger triangular floaters with an edge length 1948 m at the center surrounded by 80 smaller triangular floaters with edge length 0.948 m. All floaters had a draft of 0.0357 m. The structure was subjected to 3 different irregular wave conditions with significant wave height H_s ranging between 0.0149 m and 0.062 m and peak period T_p between 0.52 s and 0.91 s to investigate the motion response and the wave-induced loads on the structure. They considered the structure at model scale and extrapolated the results to three different full-scale dimensions. They concluded that loads on large full-scale structures are very high, leading to challenges for future applications of this mega islands at sea.

The focus of the aforementioned studies was on the motion response of the structures. Their results showed that VLFS deflection amplitudes were in the order of the structural thickness and the wave amplitude.

Recently, Schreier and Jacobi (2020) tested a closed-pore chloroprene foam rubber sheet of 4.95 m long, 1.02 m wide, 0.005 m thick and 0.17 m characteristic length in regular waves with wavelength 0.495 m and 0.99 m and up to 0.020 m amplitude. This structure followed the local wave elevation and thus experienced deflections of 4 times its thickness.

An overview of models used in VLFS experiments is provided in Table 4.

3.2.3. Ice-related structures

In ice-related experiments, early work can be found in Squire (1984) where experiments were carried out in an ice-covered wave flume of 2 m by 1 m by 0.6 m for the purpose of verification of theory. Meylan (1993) conducted 2D experiments of floating flexible sheets in a wave flume of 20 m long and 1.83 m wide to investigate the effect of the model on regular waves. The models covered the full width of the flume with length of 1.22 m and thickness of 0.0032 m and 0.00635 m corresponding to a characteristic length of 0.94 m and 1.57 m, respectively. Sakai and Hanai (2002) presented an experiment using polyethylene sheets with 0.005 m and 0.020 m thickness to model the ice floe. Six different lengths from 0.25 m to 8 m were used. The characteristic length of 0.005 m thick model was 1.09 m and the other was 2.88 m. Regular waves of periods 0.6 s to 1.6 s with intervals of 0.2 s were considered. The vertical displacement of the sheets at several points along the centerline of the models were measured. Montiel et al. (2013) used compliant discs to represent ice floes. Experiments of three kinds of discs with same radius of 0.72 m and different thicknesses of 0.003 m, 0.005 m, 0.010 m with corresponding characteristic lengths of 0.76 m, 0.98 m and 1.64 m were carried out in regular waves. Bennetts and Williams (2015) experimentally investigated the wave transmission by an ice floe. The experimental tests were conducted in a 3D wave basin with size of 15.5 m by 10 m with 0.5 m water depth. Regular waves with wavelengths of 0.56 m, 1.00 m, and 1.51 m were applied. The ice floes were represented by 1 m^2 square thin elastic plates made of polyvinyl chloride (PVC) and polypropylene (PP). Different thicknesses were considered to obtain different elasticity of the model. Meylan et al. (2015) reported an experimental test of a thin plastic disc of 0.40 m diameter and 0.015 m thickness subjected to regular wave with wavelength of 0.5 to 5 m. The model was a rigid body made of a closed-cell expanded-foam PVC sheet with thin hard plastic coating, so only rigid body motions of the model was measured and presented. A regime change from a rapid increase in surge amplitude with increasing wavelength, to a weak increase was displayed in their experimental results. Toffoli et al. (2015) demonstrated a laboratory experimental model of an incident ocean wave interacting with an ice floe to validate the theoretical models of wave attenuation in the ice-covered ocean. The model floe was represented by a rectangular PP plastic plate with length of 1 m, width of 1.7 m and thickness of 0.010 m. The model plate had manufacturer-specified Young's modulus $E = 1.6$ GPa which corresponds to a characteristic length of 2.15 m. Three incident wavelengths: $\lambda = 1.00$ m, 1.26 m and 1.56 m were used. Considering wave attenuation under ice floes, Sree et al. (2017) conducted 2D experiments with viscoelastic sheets made of oil-doped Polydimethylsiloxane (PDMS) and PP in a 8 m long, 0.3 m wide and 1.0 m deep wave flume. The size of the PDMS model was 1 m by 0.3 m by 0.01 m with characteristic lengths ranging from 0.18 m to 0.3 m at lab scale. Two model lengths of 1 m and 2.45 m with a characteristic length of 2.61 m were considered in the PP model. Their experimental results displayed wave shortening under PDMS model for longer waves and wave lengthening under a stiffer PP model. Later, the response of a longer and thicker PDMS model with length of 3 m and thickness of 0.02 m was tested by Sree et al. (2018).

An overview table of models used in ice-related experiments is provided in Table 5.

4. Characterization of the structures

Studies on elastic structure hydroelasticity have mainly addressed the wave-induced structure deformation and the influence of the structure on the entire water wave field. In this section, the characterization of the structures is discussed in terms of structure response and wave reaction which is represented by the hydro-elastic dispersion relation.

4.1. Structure response

Based on VLFS research, Suzuki et al. (2006) characterized the motion of floating structures by the ratios of structure length over characteristic length L/λ_c and structure length over wavelength L/λ_w. When the structure length is less than the characteristic length, i.e., $L/\lambda_c < 1$, motion response is dominated by rigid body motions. When the

Table 5
Models used in ice-related experiments.

$L \times B \times h$ [m^3]	λ_c [m]	λ [m]	Reference
$1.22 \times 1.83 \times 0.0032,\ 0.00635$	0.94, 1.57	0.56 – 6.25	Meylan (1993)
$8.00 \times 0.80 \times 0.005, 0.02$	1.09, 2.88	0.56 – 4.00	Sakai and Hanai (2002)
R $0.72 \times 0.003, 0.005,\ 0.01$	0.76, 0.98, 1.64	0.90 – 4.30	Montiel et al. (2013)
$1.00, 2.00, 3.00 \times 1.00 \times 0.005,\ 0.01,\ 0.02$	0.95 – 3.61	0.56 – 1.51	Bennetts and Williams (2015)
R 0.40×0.015	–	0.50 – 5.00	Meylan et al. (2015)
$1.00 \times 1.70 \times 0.01$	2.15	1.00 – 1.56	Toffoli et al. (2015)
$1.00 \times 0.30 \times 0.01$	0.18 – 0.30	0.39 – 1.37	Sree et al. (2017)
$1.00, 2.45 \times 0.30 \times 0.01$	2.61	0.39 – 1.37	Sree et al. (2017)
$3.00 \times 0.30 \times 0.01$	0.18 – 0.30	0.39 – 1.37	Sree et al. (2018)

R: the radius of the structure.

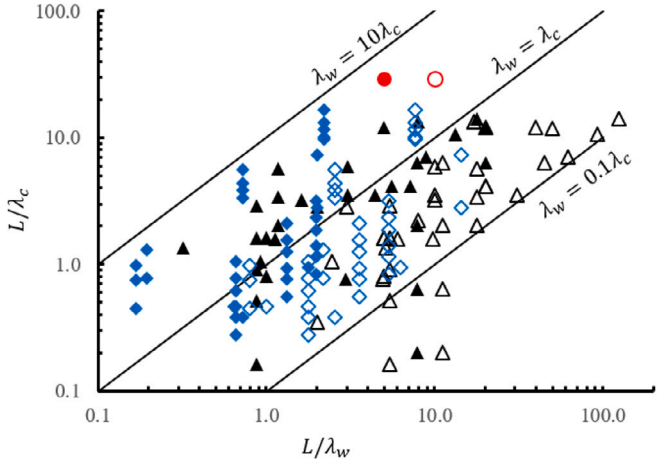

Fig. 3. Overview of characteristics of floating model structures. Black triangles: VLFS, Utsunomiya et al. (1995), Yago and Endo (1996), Ohmatsu (1997), Kagemoto et al. (1998), Liu and Sakai (2002), Shiraishi et al. (2003), Takagi and Nagayasu (2007), Pham et al. (2009), Wu et al. (1996), Kashiwagi (1997), Kim (1998), Ertekin and Kim (1999), Hong et al. (2003), Chen et al. (2003), Ohkusu and Namba (2004), Watanabe et al. (2006), Gao et al. (2011) and Tay and Wang (2012); blue diamonds: ice-related structures, Meylan (1993), Sakai and Hanai (2002), Montiel et al. (2013), Bennetts and Williams (2015), Toffoli et al. (2015) and Sree et al. (2017, 2018), red circles: more flexible structure, Schreier and Jacobi (2020). Solid and hollow points represent the longest and shortest wavelengths used in each paper. (For interpretation of the references to color in this figure legend, the reader is referred to the web version of this article.)

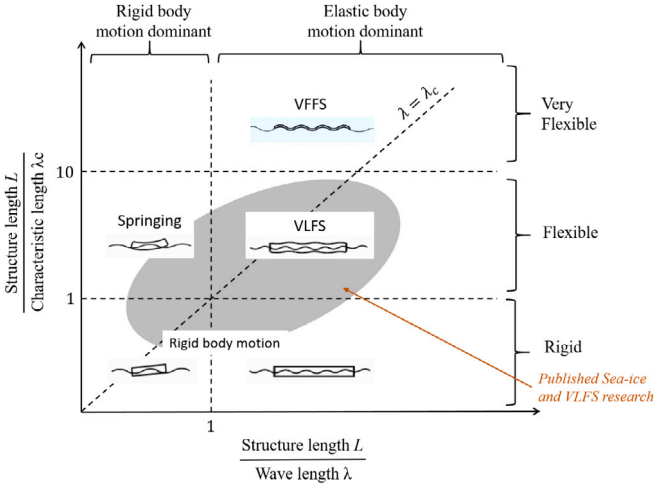

Fig. 4. Mapping of global response of floating structures.
Source: Adapted from Suzuki et al. (2006).

structure length exceeds the characteristic length, i.e. $L/\lambda_c > 1$, elastic deflections of the structure become more pronounced. The ratio of λ_w/λ_c determines the magnitude of the global response. When the waves are longer than the characteristic length, i.e. $\lambda_w/\lambda_c > 1$, the global response becomes significant, otherwise the response is small due to the cancellation of local wave effects in the range of the characteristic length λ_c.

Following this approach, an overview of characteristics of the elastic models used in the literature mentioned in Section 3 is given in Fig. 3. In this figure, the ratio L/λ_c is plotted against the ratio L/λ_w, both on logarithmic scales. The higher the structure is on the vertical axis, the more flexible it is. On the other hand, the further a structure is on the right on the horizontal axis, the longer the structure is compared to the waves. The three diagonal lines indicate from top to bottom the ratio of wavelength to structure characteristic length $\lambda_w/\lambda_c = 10; 1; 0.1$. The black triangle symbols in the figure represent VLFS, while blue diamonds show sea-ice related structures. The solid and open symbols indicate longest and shortest wavelength per study, respectively. The two red circles show the characteristic of the structure used by Schreier and Jacobi (2020).

From Fig. 3, we can see that VLFS were mostly investigated in the ranges of $1 < L/\lambda_w < 20$ and $0.1 < L/\lambda_c < 10$ with few exceptions of very short waves with L/λ up to 100. Ice-related structures share the same range of L/λ_c with VLFS but were tested for smaller length to wavelength ratios L/λ_w from 0.1 to 10. For almost all VLFS and most ice-related structures, the structure was longer than the wavelength, such that elastic body response was dominant over rigid body motions. On the other hand, for a large group of ice-related structures, the structure was shorter than the characteristic length and the response of the simulated ice-floes could be expected to be well described by rigid body motions. The ratio of wavelength to characteristic lengths λ_w/λ_c of VLFS and sea-ice models were similar and ranged from 0.1 to 10. Note that $\lambda_w/\lambda_c < 1$ for most models subjected to short waves, i.e. on the right hand side of the figure. For these floating structures, only small global response may be expected. The model in this figure used by Schreier and Jacobi (2020) had the largest ratio of $L/\lambda_c = 29.12$ which was almost three times the largest L/λ_c in VLFS and sea-ice. This suggested a significant flexible response of the structure. Schreier and Jacobi (2020) observed that their flexible model followed local wave elevation and reported a large motion amplitude for this structure of four times the structural thickness.

Following the map of structural response regions by Suzuki et al. (2006), Fig. 4 presents an updated map that indicates the difference in structure response of floating structures based on the overview data in Fig. 3. As the more flexible structures of Schreier and Jacobi (2020) had significantly larger deflection compared to structural thickness than traditional VLFS and ice-related structures, it is reasonable to introduce the new category of Very Flexible Floating Structures (VFFS) and separate these from VLFS and sea-ice.

Regarding the characteristic length λ_c, Suzuki et al. (2006) illustrated the difference in behavior of a rigid body represented by a conventional ships and an elastic one like a VLFS. They concluded that the applied load only had influence on the elastic deformation within the region of λ_c. To account for the more flexible structure investigated by Schreier and Jacobi (2020), this figure by Suzuki et al. (2006) was updated in Fig. 5.

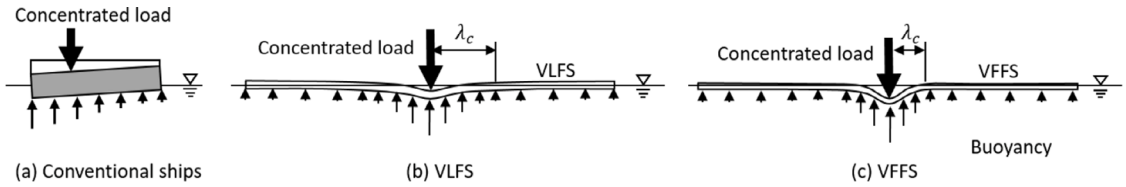

Fig. 5. Global response under a static load.
Source: Adapted from Suzuki et al. (2006).

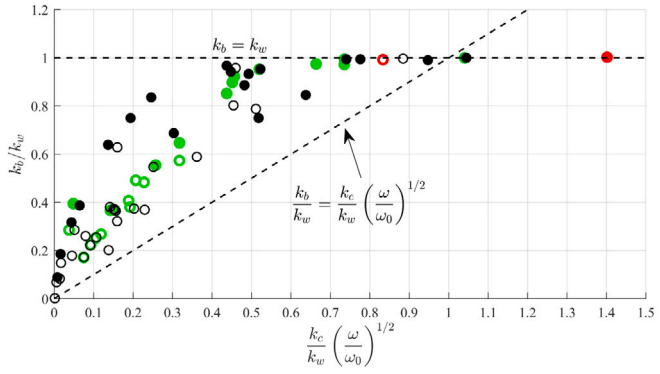

Fig. 6. Overview of wave response under elastic floating structures, black circles: numerical results, Fox and Squire (1991), Meylan and Squire (1994), Utsunomiya et al. (1995), Wu et al. (1995), Meylan and Squire (1996), Wu et al. (1996, 1997), Kagemoto et al. (1998), Kim et al. (2005), Tay and Wang (2012), Karperaki et al. (2015) and Lu et al. (2016); green circles: experimental results, Utsunomiya et al. (1995), Ohmatsu (1997), Hamamoto and Fujita (2002), Liu and Sakai (2002), Shiraishi et al. (2003), Li et al. (2003) and Toffoli et al. (2015); red circles: experimental results of more flexible structure, Schreier and Jacobi (2020). Solid and hollow points represent the longest and shortest wavelengths used in each paper. (For interpretation of the references to color in this figure legend, the reader is referred to the web version of this article.)

4.2. Hydroelastic dispersion relation

Based on the analysis in Section 2, the hydro-elastic wave number is determined by the two dimensionless parameters: $(\omega/\omega_0)^2$ and $(k_b/k_c)^4$ which relate to structural properties and incident wave conditions. Rewriting the condition of wave shortening by $k_b < k_c\left(\frac{\omega}{\omega_0}\right)^{1/2}$ and combining the relation $k_b > k_w$, wave shortening can be further expressed as $1 < \frac{k_b}{k_w} < \frac{k_c}{k_w}(\frac{\omega}{\omega_0})^{1/2}$. Similarly, wave lengthening as $\frac{k_c}{k_w}(\frac{\omega}{\omega_0})^{1/2} < \frac{k_b}{k_w} < 1$. Fig. 6 illustrates wave response under floating elastic structures in terms of $\frac{k_b}{k_w}$ and $\frac{k_c}{k_w}(\frac{\omega}{\omega_0})^{1/2}$.

From Fig. 6, we can see that almost all conditions used in the open literature are in the range of $\frac{k_c}{k_w}(\frac{\omega}{\omega_0})^{1/2} < \frac{k_b}{k_w} < 1$. This agrees with the conclusion that VLFS often cause wave lengthening, as documented by (e.g. Kashiwagi, 1998c,b; Ertekin and Kim, 1999). A few cases sit in the range of $\frac{k_b}{k_w} < \frac{k_c}{k_w}(\frac{\omega}{\omega_0})^{1/2}$, like the experimental case of Utsunomiya et al. (1995) (the upper right solid black and green points, the two models here are actually the same) and Schreier and Jacobi (2020) (the upper right solid red circle), indicating that wave may be shortened by the floating structures. But as shown in Fig. 6 the hydro-elastic wave number (k_b) of these models is very close to the open water wave number (k_w), the wavelength change is too small to be detected.

Wave lengthening and shortening are also documented in ice-related studies, see (e.g. Wang and Shen, 2010; Li et al., 2015; Sree et al., 2017, 2018). In the analysis of dispersion relation of ice structures, viscous effect is often considered and a viscous term is admitted. This viscous term can be regarded as an extra term added on $(\frac{\omega}{\omega_0})^2$, thus increasing the possibility of wave shortening.

For a VFFS, the structure is thin and flexible, the characteristic wave number of the structure could be very large compared to a VLFS, resulting in rather small $(\frac{k_b}{k_c})^4$, which also increase the possibility of wave shortening.

5. Discussion of applicable theory for VFFS analysis

As summarized in Section 4, VFFS have a large structure length to characteristic length ratio, resulting in significant elastic body motions in global response to external wave loads with large deflection amplitudes compared to their structural thickness. However, no dedicated VFFS theory exists, yet. Therefore, in this section, the applicability and limitations of classical thin plate theory to VFFS is discussed.

Commonly, VLFS and sea-ice hydroelastic analysis is based on thin (Kirchhoff) plate theory, as shown in Eq. (1).

It is worth noting that the thin plate theory gives good results for small rotations only (<10°). In case of large-amplitude motion, extended formulations accounting into geometric non-linearity must be used (Irschik and Gerstmayr, 2009; Jang, 2013; Chen et al., 2003). In this regard, an extra nonlinear membrane force term induced by large deflections is added in the equilibrium relation of the elastic model

$$D\nabla^4 W + m\frac{\partial^2 W}{\partial t^2} + \rho g W - \left(N_{xx}\frac{\partial^2 W}{\partial x^2} + N_{yy}\frac{\partial^2 W}{\partial y^2} + 2N_{xy}\frac{\partial^2 W}{\partial x \partial y}\right) = P \quad (9)$$

with N_{xx}, N_{yy} being the in-plane normal stresses in x and y directions respectively, and N_{xy} the in-plane torsional stress. More details of their calculation can be found in Reddy (2006).

This equation, which was firstly introduced by Föppl (1897) and further modified by von Kármán (1907), can be seen as an extension of classic plate theory to problems of large deflections involving moderately large rotations (10° − 15°). The derivation follows the Kirchhoff hypothesizes, which assume line elements perpendicular to the transverse normals remains straight after deformation and transverse normals are in-extensible (Reddy, 2006). Due to moderate rotation, the effect of higher-order strains, mainly $(\frac{\partial W}{\partial x})^2$, $(\frac{\partial W}{\partial y})^2$ and $(\frac{\partial W}{\partial x})(\frac{\partial W}{\partial y})$ which are neglected in thin plate theory, are no longer small enough to be neglected. Hence membrane forces play a role in the structure behavior.

Chen et al. (2003) considered the effect of membrane forces on the motion of a pontoon VLFS subjected to short waves using Föppl–von Kármán equations. They reported that the membrane forces increased the longitudinal stresses by 30% and hence should be considered in the design procedure of such structures.

The key element of VFFS analysis is the large deflection of the structure compared to its thickness and horizontal dimensions. Schreier and Jacobi (2020) have shown that their VFFS model could follow the local wave elevation. Therefore, the structure deflection can be approximated by the undisturbed wave elevation. Based on their conclusion, we express the plate motion by the time-harmonic model of free surface wave to easily calculate the value of the four terms in the left-hand side in Eq. (9) and quantify the effect of the membrane term on the hydro-elastic response. Considering head incident wave, the wave elevation is thus given as

$$W(x,t) = \xi_a \cos(k_w x - \omega t) \quad (10)$$

where ξ_a is the incident wave amplitude. Substituting Eq. (10) into Eq. (9), the four terms in the left-hand side in Eq. (9) of the VFFS model can be obtained. Leaving out the time and space dependency,

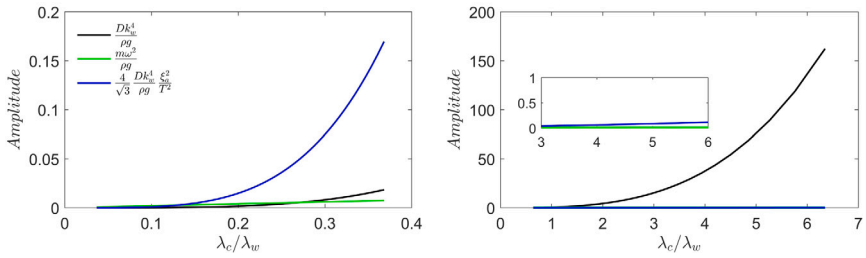

(a) VFFS (b) VLFS

Fig. 7. Normalized amplitudes of the left-hand side terms in Eq. (9) versus λ_c/λ_w. (a) VFFS model (Schreier and Jacobi, 2020): structure displacement is assumed to be equal to the wave elevation amplitude. (b) VLFS model (Yago and Endo, 1996): structure displacement is considered to linearly vary from 0.1 to 0.8 with $\lambda_w/L = 0.1 - 1.0$. Wave amplitude $\xi_a = 0.01$ m is used in both models and wavelength change underneath is ignored.

the resulting amplitudes of the individual terms are $Dk_w^4\xi_a$, $m\omega^2\xi_a$, $\rho g\xi_a$ and $\frac{4D}{\sqrt{3}T^2}k_w^4\xi_a^3$ with T the structure thickness. Normalizing those terms by hydrostatic stiffness term $\rho g\xi_a$ leads to $\frac{Dk_w^4}{\rho g}$, $\frac{m\omega^2}{\rho g}$, and $\frac{4}{\sqrt{3}}\frac{Dk_w^4}{\rho g}\frac{\xi_a^2}{T^2}$, which are all dimensionless.

Fig. 7 illustrates the non-dimensional amplitudes varying with λ_c/λ_w of a VFFS model (Schreier and Jacobi, 2020) and a VLFS model (Yago and Endo, 1996). In this figure, $\xi_a = 0.01$ m and $\lambda_w/L = 0.1 - 1.0$ is used. The results of a VLFS model (Yago and Endo, 1996) is depicted for the purpose of comparison. Note that those values of VLFS are also achieved using Eq. (10) by assuming that the VLFS displacements vary linearly with λ_w/L based on the displacement results given in literature. For instance, for small $\lambda_w/L = 0.1$, VLFS displacement is 0.1 times the incident wave amplitude, while for large $\lambda_w/L = 1.0$, VLFS displacement is 0.8 times the incident wave amplitude. So the non-dimensional amplitude of the hydro-elastic term of the VLFS model is 0.1–0.8 with $\lambda_w/L = 0.1 - 1.0$. Wavelength change underneath the structure is ignored.

From Fig. 7, we can see that the bending term is the dominant one in VLFS, while in VFFS, the hydrostatic term, which value is 1 in Fig. 7(a), is the most important one. The mass related term increases with a decrease in incident wavelength and the amplitude is rather small compared to the dominant term in both models. The magnitude of the membrane related term also increases when the incident wavelength becomes shorter. However, compared to the dominant term, this membrane term is still very small in VLFS, so the effect of this term is often neglected in most VLFS research. Whereas in VFFS, the membrane term could be much larger than the stiffness term when the structure is subjected to short waves. Therefore, including bending stiffness while neglecting membrane stiffness in VFFS research would miss important physics. Worth mentioning that Fig. 7 only shows the results of a very small wave amplitude. For larger wave amplitude, the amplitude of the structure stiffness term and the mass term would not change because the non-dimensional representation of these two terms are independent on the wave amplitude However, the amplitude of the membrane term would increase significantly with increasing wave amplitude as the dimensionless membrane term still relates to the square of the wave amplitude.

Additionally, as VFFS mainly follows local wave motion, the rotation of the mid-surface normal could be approximated by the slope of the wave surface. The maximum wave slope s_{max} is the amplitude of the spatial derivative of the wave, i.e. $s_{max} = 2\pi A/\lambda$ with the wave amplitude A and wavelength λ. Introducing the wave steepness $S = H/\lambda = 2A/\lambda$, the maximum slope becomes $s_{max} = \pi S$. According to the upper limit of the mid-surface normal rotation in Kirchhoff plate theory and Föppl–von Kármán equations, the maximum wave steepness covered by Kirchhoff plate theory is $S = 0.056$, while Föppl–von Kármán plate theory is applicable up to $S = 0.083$. The wave steepness in the experiments of Schreier and Jacobi (2020) was $S = 0.04$, which is well within the applicability of Kirchhoff plate theory. However, the theoretical breaking limit of steep waves is close to $S = 1/7 = 0.143$. Therefore, it is desirable to extend the hydroelastic analysis of VFFS to include the geometric nonlinearities of the structure and use Föppl–von Kármán plate theory.

6. Conclusions

Studies of continuous flexible floating structures were reviewed with focus on the employed experimental and numerical models and methods. Based on the motion response characteristics as well as the ratio of structure length to characteristic length, the new category of Very Flexible Floating Structures (VFFS) was introduced. VFFS are envisaged as floating support structures for Offshore Floating Photovoltaic (OFPV) installations. For the design of such structure, the prediction of motion response in waves is essential. The main conclusions of this work are summarized below.

1. VFFS have much smaller characteristic length than traditional pontoon-type VLFS and ice-related structures, indicating larger structure deflections than those two.
2. Wave shortening is probable to happen under VFFS when considering a very small characteristic length of the structure.
3. Membrane forces are shown to be much more relevant in VFFS compared to VLFS and therefore need to be considered for VFFS simulations. The Föppl–von Kármán plate theory should be used to take the geometric nonlinearities and resulting membrane forces induced by larger structure deformations into account.

Declaration of competing interest

The authors declare that they have no known competing financial interests or personal relationships that could have appeared to influence the work reported in this paper.

Data availability

Data of Figures 3 and 6 will be made available on request.

Acknowledgments

This work is financially supported by China Scholarship Council (No. 2018069 50099).

References

Abul-Azm, A.G., Gesraha, M.R., 2000. Approximation to the hydrodynamics of floating pontoons under oblique waves. Ocean Eng. 27 (4), 365–384. http://dx.doi.org/10.1016/S0029-8018(98)00057-2.

Andrianov, A.I., 2005. Hydroelastic Analysis of Very Large Floating Structures (Doctoral Thesis). Delft University of Technology.

Andrianov, A.I., Hermans, A.J., 2006. Hydroelastic analysis of a floating plate of finite draft. Appl. Ocean Res. 28 (5), 313–325.

Athanassoulis, G., Belibassakis, K., 1999. A consistent coupled-mode theory for the propagation of small-amplitude water waves over variable bathymetry regions. J. Fluid Mech. 389, 275–301.

Belibassakis, K., Athanassoulis, G., 2005. A coupled-mode model for the hydroelastic analysis of large floating bodies over variable bathymetry regions. J. Fluid Mech. 531, 221.

Belibassakis, K., Athanassoulis, G., Gerostathis, T.P., 2013. Hydroelastic analysis of very large floating bodies over variable bathymetry regions. In: 10th HSTAM International Congress on Mechanics. Chania, Crete, Greece.

Bennetts, L., Williams, T., 2015. Water wave transmission by an array of floating discs. Proc. R. Soc. A 471 (2173), 20140698.

Bishop, R.E.D., Bishop, R.E., Price, W., 1979. Hydroelasticity of Ships. Cambridge University Press.

Chen, X.J., Jensen, J.J., Cui, W.C., Fu, S.X., 2003. Hydroelasticity of a floating plate in multidirectional waves. Ocean Eng. 30 (15), 1997–2017. http://dx.doi.org/10.1016/S0029-8018(03)00020-9.

Chen, X.J., Juncher, J.J., Cui, W.C., Tang, X.F., 2004. Hydroelastic analysis of a very large floating plate with large deflections in stochastic seaway. Mar. Struct. 17 (6), 435–454. http://dx.doi.org/10.1016/j.marstruc.2004.12.001.

Cheng, Y., Ji, C., Zhai, G., Gaidai, O., 2016. Hydroelastic analysis of oblique irregular waves with a pontoon-type VLFS edged with dual inclined perforated plates. Mar. Struct. 49, 31–57.

Ding, J., Wu, Y.-s., Zhou, Y., Ma, X.-Z., Ling, H.J., Xie, Z., 2020. Investigation of connector loads of a 3-module VLFS using experimental and numerical methods. Ocean Eng. 195, 106684.

Endo, H., 1991. The laws of similitude in hydroelasticity problems first report: Derivation of laws of similitude. J. Soc. Nav. Archit. Jpn. 1991 (169), 347–354.

Ertekin, R.C., Kim, J.W., 1998. A parametric study of the hydroelastic response of a floating, mat-type runway in regular waves. In: IEEE Oceanic Engineering Society. OCEANS'98. Conference Proceedings (Cat. No. 98CH36259), Vol. 2. IEEE, pp. 988–992.

Ertekin, R.C., Kim, J.W., 1999. Hydroelastic response of a floating mat-type structure in oblique, shallow-water waves. J. Sh. Res. 43 (4), 241–254.

Evans, D.V., Davies, T.V., 1968. Wave-Ice Interaction. Technical Report, Stevens Inst of Tech Hoboken NJ Davidson Lab.

Föppl, A., 1897. Vorlesungen Über Technische Mechanik, Vol. 3. BG Teubner.

Fox, C., Squire, V.A., 1991. Coupling between the ocean and an ice shelf. Ann. Glaciol. 15, 101–108.

Gao, R.P., Tay, Z.Y., Wang, C.M., Koh, C.G., 2011. Hydroelastic response of very large floating structure with a flexible line connection. Ocean Eng. 38 (17–18), 1957–1966. http://dx.doi.org/10.1016/j.oceaneng.2011.09.021.

Georgiadis, C., 1981. Wave Induced Vibrations of Continuous Floating Structures (Doctoral Thesis). University of Washington.

Gran, S., 1992. A Course in Ocean Engineering. Elsevier, Amsterdam.

Hamamoto, T., Fujita, K., 2002. Wet-mode superposition for evaluating the hydroelastic response of floating structures with arbitrary shape. In: The Twelfth International Offshore and Polar Engineering Conference. pp. 290–297.

Hamamoto, T., Suzuki, A., Fujita, K.-i., et al., 1997. Hybrid dynamic analysis of large tension leg floating structures using plate elements. In: The Seventh International Offshore and Polar Engineering Conference. International Society of Offshore and Polar Engineers.

Hegarty, G.M., Squire, V.A., 2008. A boundary-integral method for the interaction of large-amplitude ocean waves with a compliant floating raft such as a sea-ice floe. J. Eng. Math. 62 (4), 355–372.

Heo, K., Kashiwagi, M., 2019. A numerical study of second-order springing of an elastic body using higher-order boundary element method (HOBEM). Appl. Ocean Res. 93, 101903.

Heo, K., Kashiwagi, M., 2020. Numerical study on the second-order hydrodynamic force and response of an elastic body–In bichromatic waves. Ocean Eng. 217, 107870.

Hermans, A.J., 2000. A boundary element method for the interaction of free-surface waves with a very large floating flexible platform. J. Fluids Struct. 14 (7), 943–956. http://dx.doi.org/10.1006/jfls.2000.0313, URL: https://linkinghub.elsevier.com/retrieve/pii/S088997460090313X.

Hong, S.Y., Kim, J.W., Ertekin, R.C., Shin, Y.S., 2003. An eigenfunction-expansion method for hydroelastic analysis of a floating runway. In: The Thirteenth International Offshore and Polar Engineering Conference. pp. 121–128.

Irschik, H., Gerstmayr, J., 2009. A continuum mechanics based derivation of Reissner's large-displacement finite-strain beam theory: the case of plane deformations of originally straight Bernoulli–Euler beams. Acta Mech. 206 (1), 1–21.

Jamalludin, M.A.S., Muhammad-Sukki, F., Abu-Bakar, S.H., Ramlee, F., Munir, A.B., Bani, N.A., Muhtazaruddin, M.N., Mas' ud, A.A., Ardila-Rey, J.A., Ayub, A.S., et al., 2019. Potential of floating solar technology in Malaysia. Int. J. Power Electron. Drive Syst. (IJPEDS) 10 (3).

Jang, T.S., 2013. A new semi-analytical approach to large deflections of Bernoulli-Euler-v. Karman beams on a linear elastic foundation: Nonlinear analysis of infinite beams. Int. J. Mech. Sci. 66, 22–32. http://dx.doi.org/10.1016/j.ijmecsci.2012.10.005.

Jiang, D., Tan, K.H., Dai, J., Ang, K.K., Nguyen, H.P., 2021. Behavior of concrete modular multi-purpose floating structures. Ocean Eng. 229, 108971.

Kagemoto, H., Fujino, M., Murai, M., 1998. Theoretical and experimental predictions of the hydroelastic response of a very large floating structure in waves. Appl. Ocean Res. 20 (3), 135–144.

Karmakar, D., Soares, C.G., 2012. Scattering of gravity waves by a moored finite floating elastic plate. Appl. Ocean Res. 34, 135–149.

von Kármán, T., 1907. Festigkeitsprobleme im maschinenbau. In: Mechanik. Springer, pp. 311–385.

Karperaki, A.E., Belibassakis, K.A., Papathanasiou, T.K., Markiloefas, S.I., 2015. Higher-order FEM for nonlinear hydroelastic analysis of a floating elastic strip in shallow-water conditions. In: COUPLED VI: Proceedings of the VI International Conference on Computational Methods for Coupled Problems in Science and Engineering. CIMNE, pp. 1110–1122.

Kashiwagi, M., 1997. A B-spline Galerkin scheme for computing wave forces on a floating very large elastic plate. In: The Seventh International Offshore and Polar Engineering Conference. pp. 229–236.

Kashiwagi, M., 1998a. A B-spline Galerkin scheme for calculating the hydroelastic response of a very large floating structure in waves. J. Mar. Sci. Technol. 3 (1), 37–49. http://dx.doi.org/10.1007/BF01239805.

Kashiwagi, M., 1998b. A direct method versus a mode-expansion method for calculating hydroelastic response of a VLFS in waves. In: The Eighth International Offshore and Polar Engineering Conference. pp. 215–222.

Kashiwagi, M., 1998c. A new direct method for calculating hydroelastic deflection of a very large floating structure in waves. In: 13th International Worshop on Water Waves and Floating Bodies, Alphen Aan Den Rijn, Netherland.

Kim, J.W., 1998. An eigenfunction expansion method for predicting hydroelastic behavior of a shallow-draft VLFS. In: Proc. 2nd Intl. Conf. on Hydroelasticity in Marine Tech., Fukuoka, 1998, pp. 47–59.

Kim, J.W., Ertekin, R.C., 2000. Hydroelastic response of mat-type VLFS: Effects of non-zero draft and mass assumptions. In: OCEANS 2000 MTS/IEEE Conference and Exhibition. Conference Proceedings (Cat. No. 00CH37158), Vol. 1. IEEE, pp. 541–547.

Kim, B.W., Kyoung, J.H., Hong, S.Y., Cho, S.K., 2005. Investigation of the effect of stiffness distribution and structure shape on hydroelastic responses of very large floating structures. In: The Fifteenth International Offshore and Polar Engineering Conference. Seoul, pp. 210–217.

Lamas-Pardo, M., Iglesias, G., Carral, L., 2015. A review of Very Large Floating Structures (VLFS) for coastal and offshore uses. Ocean Engineering 109, 677–690. http://dx.doi.org/10.1016/j.oceaneng.2015.09.012.

Langen, I., Sigbjörnsson, R., 1980. On stochastic dynamics of floating bridges. Eng. Struct. 2 (4), 209–216.

Li, J., Mondal, S., Shen, H.H., 2015. Sensitivity analysis of a viscoelastic parameterization for gravity wave dispersion in ice covered seas. Cold Reg. Sci. Technol. 120, 63–75. http://dx.doi.org/10.1016/j.coldregions.2015.09.009.

Li, R., Shu, Z., Wang, Z., 2003. A numerical and experimental study on the hydroelastic behavior of the box-typed very large floating structure in waves. In: The Thirteenth International Offshore and Polar Engineering Conference. International Society of Offshore and Polar Engineers.

Liu, X., Sakai, S., 2002. Time domain analysis on the dynamic response of a flexible floating structure to waves. J. Eng. Mech. 128 (1), 48–56.

López, M., Rodríguez, N., Iglesias, G., 2020. Combined floating offshore wind and solar PV. J. Mar. Sci. Eng. 8 (8), 576.

Loukogeorgaki, E., Michailides, C., Angelides, D.C., 2012. Hydroelastic analysis of a flexible mat-shaped floating breakwater under oblique wave action. J. Fluids Struct. 31, 103–124. http://dx.doi.org/10.1016/j.jfluidstructs.2012.02.011.

Lu, D., Fu, S., Zhang, X., Guo, F., Gao, Y., 2016. A method to estimate the hydroelastic behaviour of VLFS based on multi-rigid-body dynamics and beam bending. Ships Offshore Struct. 14 (4), 354–362.

Luong, V.H., Nguyen, X.V., Cao, T.N.T., Tran, M.T., Nguyen, H.P., 2020. A time-domain 3D BEM–MEM method for flexural motion analyses of floating Kirchhoff plates induced by moving vehicles. Int. J. Struct. Stab. Dyn. 20 (03), 2050041.

Maeda, H., Ikoma, T., Masuda, K., Rheem, C.-K., 2000. Time-domain analyses of elastic response and second-order mooring force on a very large floating structure in irregular waves. Mar. Struct. 13 (4–5), 279–299.

Maeda, H., Masuda, K., Miyajima, S., Ikoma, T., 1995. Hydroelastic responses of pontoon type very large floating offshore structure. J. Soc. Nav. Archit. Jpn. 1995 (178), 203–212.

Mamidipudi, P., Webster, W., 1994. The motion performance of a mat-like floating airport. In: Proceedings of the International Conference on Hydroelasticity in Marine Technology, Trondheim, Norway, pp. 363–375.

Mei, C.C., Tuck, E., 1980. Forward scattering by long thin bodies. SIAM J. Appl. Math. 39 (1), 178–191.

Meylan, M., 1993. The Behaviour of Sea Ice in Ocean Waves (Ph.D. thesis). University of Otago.

Meylan, M.H., 2002. Wave response of an ice floe of arbitrary geometry. J. Geophys. Res. Oceans 107 (C1), 1–11. http://dx.doi.org/10.1029/2000jc000713.

Meylan, M.H., 2021. Time-dependent motion of a floating circular elastic plate. Fluids 6 (1), 29.

Meylan, M., Bennetts, L., Cavaliere, C., Alberello, A., Toffoli, A., 2015. Experimental and theoretical models of wave-induced flexure of a sea ice floe. Phys. Fluids 27 (4), 041704.

Meylan, M., Squire, V.A., 1994. The response of ice floes to ocean waves. J. Geophys. Res. Oceans 99 (C1), 891–900.
Meylan, M.H., Squire, V.A., 1996. Response of a circular ice floe to ocean waves. J. Geophys. Res. Oceans 101 (C4), 8869–8884.
Mohapatra, S., Guedes Soares, C., 2016. Effect of submerged horizontal flexible membrane on moored floating elastic plate. Marit. Technol. Eng. 3, 1181–1188.
Mohapatra, S., Soares, C.G., 2019. Interaction of ocean waves with floating and submerged horizontal flexible structures in three-dimensions. Appl. Ocean Res. 83, 136–154.
Montiel, F.F., 2012. Numerical and Experimental Analysis of Water Wave Scattering by Floating Elastic Plates (Ph.D. thesis). University of Otago.
Montiel, F., Bonnefoy, F., Ferrant, P., Bennetts, L., Squire, V., Marsault, P., 2013. Hydroelastic response of floating elastic discs to regular waves. Part 1. Wave basin experiments. J. Fluid Mech. 723 (1), 604–628.
Newman, J.N., 1994. Wave effects on deformable bodies. Appl. Ocean Res. 16 (1), 47–59. http://dx.doi.org/10.1016/0141-1187(94)90013-2.
Nguyen, X.V., Luong, V.H., Cao, T.N.T., Lieu, X.Q., Nguyen, T.B., 2020. Hydroelastic responses of floating composite plates under moving loads using a hybrid moving element-boundary element method. Adv. Struct. Eng. 23 (13), 2759–2775.
Ocean Sun, 2018. Kyrholmen. https://oceansun.no/project/kyrholmen.
Oceans of Energy, 2019. North sea offshore solar project. https://oceansofenergy.blue/north-sea-1-offshore-solar-project.
Ohkusu, M., Namba, Y., 2004. Hydroelastic analysis of a large floating structure. J. Fluids Struct. 19 (4), 543–555. http://dx.doi.org/10.1016/j.jfluidstructs.2004.02.002.
Ohkusu, M., Nanba, M., 1996. Hydroelastic behavior of a very large floating platform in waves. In: Proceedings of 11th International Workshop on Water Waves and Floating Bodies, Hamburg, Germany.
Ohmatsu, S., 1997. Numerical calculation of hydroelastic responses of pontoon type VLFS. J. Soc. Nav. Archit. Jpn. 1997 (182), 329–340. http://dx.doi.org/10.2534/jjasnaoe1968.1997.182_329, URL: http://joi.jlc.jst.go.jp/JST.Journalarchive/jjasnaoe1968/1997.182{_}329?from=CrossRef.
Ohmatsu, S., 2005. Overview: Research on wave loading and responses of VLFS. Mar. Struct. 18 (2), 149–168. http://dx.doi.org/10.1016/j.marstruc.2005.07.004.
Ohmatsu, S., 2006. Model experiments for VLFS. In: Very Large Floating Structures. CRC Press, pp. 155–178.
Ohmatsu, S., 2008. Model experiments for VLFS. In: Wang, C.M., Watanabe, E., Utsunomiya, T. (Eds.), Very Large Floating Structures. Taylor & Francis, pp. 141–164.
Oliveira-Pinto, S., Stokkermans, J., 2020. Marine floating solar plants: An overview of potential, challenges and feasibility. In: Proceedings of the Institution of Civil Engineers-Maritime Engineering, Vol. 173. Thomas Telford Ltd, pp. 120–135.
Otto, W., Waals, O., Bunnik, T., Ceneray, C., 2020. Wave induced motions of a floating Mega Island. In: WCFS2019. Springer, pp. 173–189.
Pham, D., Wang, C.M., Bangun, E., 2009. Experimental study on anti-heaving devices for very large floating structure. IES J. A: Civ. Struct. Eng. 2 (4), 255–271.
Praveen, K.M., Karmakar, D., Soares, C.G., 2018. Hydroelastic analysis of articulated floating elastic plate based on Timoshenko–Mindlin plate theory. Ships Offshore Struct. 13, 287–301. http://dx.doi.org/10.1080/17445302.2018.1457236.
Praveen, K., Karmakar, D., Soares, C.G., 2019. Influence of support conditions on the hydroelastic behaviour of floating thick elastic plate. J. Mar. Sci. Appl. 18 (3), 295–313.
Praveen, K., Venkateswarlu, V., Karmakar, D., 2020. Hydroelastic response of floating elastic plate in the presence of vertical porous barriers. Ships Offshore Struct. 1–15.
Price, W.G., Wu, Y., 1985. Hydroelasticity of marine structures. In: Theoretical and Applied Mechanics. Elsevier, pp. 311–337.
Pu, J., Lu, D.-Q., 2022. Mitigation of hydroelastic responses in a very large floating structure by a connected vertical porous flexible barrier. Water 14 (3), 294.
Reddy, J.N., 2006. Theory and Analysis of Elastic Plates and Shells. CRC Press.
Sahu, A., Yadav, N., Sudhakar, K., 2016. Floating photovoltaic power plant: A review. Renew. Sustain. Energy Rev. 66, 815–824.
Sakai, S., Hanai, K., 2002. Empirical formula of dispersion relation of waves in sea ice. In: Ice in the Environment: Proceedings of the 16th IAHR International Symposium on Ice. pp. 327–335.
Schreier, S., Jacobi, G., 2020. Experimental investigation of wave interaction with a thin floating sheet. In: The 30th International Offshore and Polar Engineering Conference. International Society of Offshore and Polar Engineers.
Shiraishi, S., Iijima, K., Harasaki, K., 2003. Elastic response characteristics of a very large floating structure in waves moored inside a reef. J. Mar. Sci. Technol. 8 (1), 1–10.
Shirkol, A., Nasar, T., 2018. Coupled boundary element method and finite element method for hydroelastic analysis of floating plate. J. Ocean Eng. Sci. 3 (1), 19–37.
Shirkol, A.I., Nasar, T., 2019. Coupled BEM and FEM for the analysis of floating elastic plate with arbitrary shapes. Ships Offshore Struct. 14 (8), 818–828. http://dx.doi.org/10.1080/17445302.2018.1564540.
Singla, S., Sahoo, T., Martha, S., Behera, H., 2019. Effect of a floating permeable plate on the hydroelastic response of a very large floating structure. J. Eng. Math. 116 (1), 49–72.
Soppe, W., 2020. Solar@sea presentation 13.02.2020 TKI wind op zee.
Squire, V.A., 1984. A theoretical, laboratory, and field study of ice-coupled waves. J. Geophys. Res. Oceans 89 (C5), 8069–8079.
Squire, V.A., 2008. Synergies between VLFS hydroelasticity and sea-ice research. In: The Eighteenth International Offshore and Polar Engineering Conference, Vol. 8. Vancouver, BC, Canada, pp. 1–13.
Squire, V.A., 2020. Ocean wave interactions with sea ice: a reappraisal. Annu. Rev. Fluid Mech. 52, 37–60.
Sree, D.K., Law, A.W.-K., Shen, H.H., 2017. An experimental study on the interactions between surface waves and floating viscoelastic covers. Wave Motion 70, 195–208. http://dx.doi.org/10.1016/j.wavemoti.2016.08.003.
Sree, D.K., Law, A.W.-K., Shen, H.H., 2018. An experimental study on gravity waves through a floating viscoelastic cover. Cold Reg. Sci. Technol. 155 (August), 289–299. http://dx.doi.org/10.1016/j.coldregions.2018.08.013.
Suzuki, H., 2005. Overview of Megafloat: Concept, design criteria, analysis, and design. Mar. Struct. 18 (2), 111–132. http://dx.doi.org/10.1016/j.marstruc.2005.07.006.
Suzuki, H., Riggs, H., Fujikubo, M., Shugar, T., Seto, H., Yasuzawa, Y., Bhattacharya, B., Hudson, D., Shin, H., 2006. Very large floating structures. In: International Conference on Offshore Mechanics and Arctic Engineering, Vol. 42681. pp. 597–608.
Suzuki, H., Yasuzawa, Y., Fujikubo, M., Okada, S., Endo, H., Hattori, Y., Okada, H., Watanabe, Y., Morikawa, M., Ozaki, M., et al., 1997. Structural response and design of large scale floating structure. In: Proceedings of the 1997 16th International Conference on Offshore Mechanics and Arctic Engineering. Part 1-B (of 6).
Suzuki, H., Yoshida, K., 1996. Design flow and strategy for safety of very large floating structure. In: Proceedings of Int Workshop on Very Large Floating Structures, VLFS, pp. 21–27.
Takagi, K., Nagayasu, M., 2007. Ray theory for predicting hydroelastic behavior of a very large floating structure in waves. Ocean Eng. 34 (3–4), 362–370.
Tay, Z., Wang, C., 2012. Reducing hydroelastic response of very large floating structures by altering their plan shapes. Ocean Syst. Eng. 2 (1), 69–81.
Taylor, R.E., 2003. Wet or dry modes in linear hydroelasticity–why modes?. In: Proceedings of the 3rd International Conference on Hydroelasticity in Marine Technology, Oxford, United Kingdom, Edited By Eatock Taylor, ISBN: 0-952-62081-2, Paper: P2003-3 Proceedings.
Taylor, R.E., 2007. Hydroelastic analysis of plates and some approximations. J. Eng. Math. 58 (1–4), 267–278. http://dx.doi.org/10.1007/s10665-006-9121-7, URL: http://link.springer.com/10.1007/s10665-006-9121-7.
Taylor, R.E., Ohkusu, M., 2000. Green functions for hydroelastic analysis of vibrating free–free beams and plates. Appl. Ocean Res. 22 (5), 295–314. http://dx.doi.org/10.1016/S0141-1187(00)00018-3, URL: https://linkinghub.elsevier.com/retrieve/pii/S0141118700000183.
Toffoli, A., Bennetts, L.G., Meylan, M.H., Cavaliere, C., Alberello, A., Elsnab, J., Monty, J.P., 2015. Sea ice floes dissipate the energy of steep ocean waves. Geophys. Res. Lett. 42 (20), 8547–8554.
Trapani, K., Millar, D.L., Smith, H.C., 2013. Novel offshore application of photovoltaics in comparison to conventional marine renewable energy technologies. Renew. Energy 50, 879–888.
Trapani, K., Santafé, M.R., 2015. A review of floating photovoltaic installations : 2007 – 2013. Prog. Photovolt.: Res. Appl. 23 (4), 524–532. http://dx.doi.org/10.1002/pip.
UN, 2017. Factsheet: people and oceans. In: The Ocean Conference. pp. 1–7.
Utsunomiya, T., Watanabe, E., Wu, C., Hayashi, N., Nakai, K., Sekita, K., et al., 1995. Wave response analysis of a flexible floating structure by BE-FE combination method. In: The Fifth International Offshore and Polar Engineering Conference. International Society of Offshore and Polar Engineers.
Waals, O., Bunnik, T., Otto, W., 2018. Model tests and numerical analysis for a floating Mega Island. In: ASME 2018 37th International Conference on Ocean, Offshore and Arctic Engineering. American Society of Mechanical Engineers Digital Collection.
Wang, C.D., Meylan, M.H., 2004. A higher-order-coupled boundary element and finite element method for the wave forcing of a floating elastic plate. J. Fluids Struct. 19 (4), 557–572. http://dx.doi.org/10.1016/j.jfluidstructs.2004.02.006.
Wang, R., Shen, H.H., 2010. Gravity waves propagating into an ice - covered ocean : A viscoelastic model. J. Geophys. Res. Oceans 115 (C6), 1–12. http://dx.doi.org/10.1029/2009JC005591.
Wang, C.M., Tay, Z.Y., 2011. Very large floating structures: Applications, research and development. Procedia Eng. 14, 62–72. http://dx.doi.org/10.1016/j.proeng.2011.07.007.
Watanabe, E., Utsunomiya, T., Wang, C.M., Hang, L.T.T., 2006. Benchmark hydroelastic responses of a circular VLFS under wave action. Eng. Struct. 28 (3), 423–430. http://dx.doi.org/10.1016/j.engstruct.2005.08.014.
Wu, Y., 1984. Hydroelasticity of Floating Bodies (Ph.D. thesis). University of Brunel.
Wu, Y., Du, S., 1990. Directly analysis method of marine structures—Random analysis theory and its application of three-dimensional hydroelasticity. Ship Behav. Res.4 (in Chinese).
Wu, G., Taylor, R.E., 2003. The coupled finite element and boundary element analysis of nonlinear interactions between waves and bodies. Ocean Eng. 30 (3), 387–400.
Wu, C., Utsunomiya, T., Watanabe, E., 1996. Application of Galerkin's method in wave response analysis of flexible floating plates. In: Proceedings of the International Offshore and Polar Engineering Conference, Vol. 3, pp. 307–314.
Wu, C., Utsunomiya, T., Watanabe, E., 1997. Harmonic wave response analysis of elastic floating plates by modal superposition method. Struct. Eng./Earthq. Eng. 14 (1), 43–52. http://dx.doi.org/10.2208/jscej.1997.556_43.

Wu, C., Watanabe, E., Utsunomiya, T., 1995. An eigenfunction expansion-matching method for analyzing the wave-induced responses of an elastic floating plate. Appl. Ocean Res. 17 (5), 301–310. http://dx.doi.org/10.1016/0141-1187(95)00023-2.

Yago, K., 1997. Model experiment and numerical calculation of the hydroelastic behavior of matlike VLFS. In: Proc. of International Workshop on VLFS, pp. 209–216.

Yago, K., Endo, H., 1996. On the hydoroelastic response of box-shaped floating structure with shallow draft. J. Soc. Nav. Archit. Jpn. 1996 (180), 341–352. http://dx.doi.org/10.2534/jjasnaoe1968.1996.180_341.

Yang, P., Liu, X., Wang, Z., Zong, Z., Tian, C., Wu, Y., 2019. Hydroelastic responses of a 3-module VLFS in the waves influenced by complicated geographic environment. Ocean Eng. 184, 121–133.

Yasuzawa, Y., 1996. Wave response analysis of a flexible large floating structure. In: Proc Int Workshop on Very Large Floating Structures (Hayama), 1996.

Yoon, J.S., Cho, S.P., Jiwinangun, R.G., Lee, P.S., 2014. Hydroelastic analysis of floating plates with multiple hinge connections in regular waves. Mar. Struct. 36, 65–87. http://dx.doi.org/10.1016/j.marstruc.2014.02.002.

Zheng, X., Zheng, H., Lei, Y., Li, Y., Li, W., 2020. An offshore floating wind–solar–aquaculture system: concept design and extreme response in survival conditions. Energies 13 (3), 604.